Nuclear magnetic shielding and chirality. I. The shielding tensor of Xe interacting with Ne helices

Devin N. Sears and Cynthia J. Jameson
Department of Chemistry M/C-111, University of Illinois at Chicago, Chicago, Illinois 60607-7061

Robert A. Harris
Department of Chemistry, University of California, Berkeley, California 94720

(Received 24 February 2003; accepted 5 May 2003)

Chirality and, in particular, induced chirality is investigated using Xe interacting with chirally perturbed Ne helices. The full nuclear magnetic shielding tensors are calculated and physical implications are discussed. © *2003 American Institute of Physics.* [DOI: 10.1063/1.1586698]

I. INTRODUCTION

There are two measures of chirality. These measures of chirality are pseudoscalar and scalar measures, respectively. A pseudoscalar measure of chirality is one that (in three dimensions) is invariant with respect to rotations, but changes sign under inversion. A scalar measure of chirality is one in which one measures an interaction between two chiral systems. The measurement is not signed but differs depending on the enantiomer. Most, but not all, pseudoscalar measurements are obtained from a combination of scalar measurements.

The simplest direct pseudoscalar measurements are optical rotation and coherent sum-frequency generation. The simplest pseudoscalar measurement that is constructed from scalar measurements is circular dichroism. The above measures of chirality, with the exception of coherent sum-frequency generation, all involve circularly polarized light, which is chiral.

In what follows we describe scalar measures of chirality that do not involve spin as the agent of chirality. Scalar measures of chirality require at least *two* chiral systems and do not vanish if one or both of the systems is achiral, the hallmark of pseudoscalar measures.

In order to be clear we shall use as examples diastereomers, by which we mean two chiral systems localized or bound to one another such that we may replace either or both with their enantiomeric twin.[1] We call one system's chirality as being L or R, the other being l or r. Hence the diastereomers are (Ll, Rr, Rl, Lr). Ll and Rr are mirror images. Rl and Lr are mirror images. From parity conservation we have for any scalar measurement (S) that

$$\mathrm{S}(Ll)=\mathrm{S}(Rr) \tag{1}$$

and

$$\mathrm{S}(Lr)=\mathrm{S}(Rl). \tag{2}$$

In general,

$$\mathrm{S}(Ll)\neq\mathrm{S}(Lr). \tag{3}$$

For pseudoscalar (PS) measurements,

$$\mathrm{PS}(Ll)=-\mathrm{PS}(Rr) \tag{4}$$

and

$$\mathrm{PS}(Rl)=-\mathrm{PS}(Lr). \tag{5}$$

In general,

$$|\mathrm{PS}(Ll)|\neq|\mathrm{PS}(Rl)| \tag{6}$$

It is clear from Eqs. (1)–(6) that one knows that Ll and Rr are mirror images and Lr and Rl are mirror images. But, the diastereomeric character is not known unless further structural information is given. If we know the systems l and r but do not know whether or not the system L (or R) is chiral, observing a split line, that is, finding the inequality (3) holds, is a necessary and sufficient condition that L or R actually is chiral. This is equivalent to the observation of + and − for pseudoscalars. As in the latter case, we cannot, without calculation or experiment, *a priori* predict which will be above or below the original line. This is true of any scalar property. Equations (1)–(3) form the basis for the application of chiral shift reagents in NMR. See, for example, Ref. 1.

In these papers we are going to investigate particular aspects of chirality and diastereomerism, namely chirality induced in an achiral system. Induction of a chiral response in an achiral molecule by a chiral environment (induced chirality) is almost as well known as chirality itself. The quantitative quantum-mechanical analysis first appeared in the work of Moffitt and Moscowitz.[2] Chirality induced in Xe has been called ''chiralization.''[3,4] An example of induced chirality has been reported in Xe trapped in cryptophane cages with chiral tethers.[5] The Pines and Wemmer groups have developed a biosensor based on a molecule designed to bind both xenon and protein.[6] The molecule consists of three parts: the cage, which contains the xenon, the ligand, which binds to the protein, and the tether, which links the ligand and the cage. The initial demonstration of the technique proved that distinct resolved xenon chemical shifts from the free and the bound molecule signal the presence and amount of the specific protein. The cryptophane cage itself is chiral; upon attaching a tether containing ℓ amino acids to solubilize the cage in water, diastereomers are produced, exhibiting induced chirality in the xenon.[5]

It is clear that the most direct measure of the additional chirality of a Xe atom interacting with a chiral system is the circular dichroism (CD) near a Xe excitation energy. The excitation energy may be determined from the absorption spectrum of the complex. Another way is to measure scalar properties related to Xe, say. Here one needs to introduce diastereomeric interactions. In particular, there will be a splitting of the Xe nuclear magnetic resonance line. Again, we stress that it is necessary but not sufficient that such a splitting occur.

In this paper we shall investigate models of chiral systems interacting with Xe. Although only the isotropic chemical shifts have been observed in Xe complexes exhibiting induced chirality,[3–5] we shall calculate not only the chemical shifts but the full shielding tensors.

II. METHODS

The chiral shifts found in Xe trapped inside chiral cages attached to tethers with asymmetric carbon centers appear to be real and reproducible.[5] Our goal here is to study the full nuclear magnetic shielding tensor of the Xe atom in a chiral environment and also in the chiral field of other asymmetric groups. To model the chiral environment we choose helices of neon atoms with a radius of 3.260 Å and a pitch of 3.5 Å, small enough so that calculated chirality shifts are not vanishingly small. We have chosen helices consisting of 7, 8, and 15 neon atoms. Because of the reduction in symmetry which occurs when the helices contain 7 and 15 Ne, we concentrate on the Ne_8 helix. The Ne_7 and Ne_{15} helices are briefly mentioned when their inclusion is appropriate. The 8 Ne atoms are in the range 3.27–3.70 Å from the Xe nucleus. To model a second chiral field electronically coupled to the helix of neon atoms, we choose a helix with a radius of 6.3706 Å, co-axial with the helix of Ne atoms, made up of a partial charge array of 15 equally spaced positive charges (magnitude $+0.061\,953e$, that is, $\frac{1}{10}$ of the partial charge that the AMBER force field software assigns to any carbonyl-type carbon atom).[7] The Ne atoms and the positive charges are equally spaced on the inner and outer helices. The inner helix of Ne_8 is either *L* or *R* and the outer helix of charges is either *l* or *r*.

Calculations of the nuclear magnetic shielding tensor are carried out using coupled perturbation methods for a system in the presence of both an external magnetic field and a nuclear moment.[8,9] Coupled Hartree–Fock or density-functional methods provide comparable results provided the basis sets used are adequate.[10] We have used both Hartree–Fock and density-functional methods for calculating shielding tensors for the Xe atom in various intermolecular environments.[11,12] In this paper we use density-functional theory (DFT) and the popular hybrid functional B3LYP. For Xe atom we use 240 basis functions, including *f* orbitals, the same basis set as we had used earlier,[11,12] from the compilation by Partridge and Faegri, with additional polarization functions from Bishop and Cybulski.[13,14] For each Ne atom we use 77 basis functions, uncontracted (18*s* 13*p*) plus four *d* polarization functions.[13] Distributed gauge origins are implemented through the use of gauge-including atomic orbitals (GIAO) and the GAUSSIAN 98 program package was used for all calculations.[15] Counterpoise calculations were performed to correct for basis set superposition errors.[16] That is, the intermolecular shielding tensor reported in this work is obtained by taking the difference between the absolute ^{129}Xe shielding calculated in the system and that calculated using all the basis functions, but with only the electrons on the Xe atom. The latter is considered the absolute shielding of the free Xe atom under full counterpoise correction. In all cases, the counterpoise corrections were found to be negligibly small. For Xe the difference between the calculated shielding in Xe atom with and without the ghost orbitals on the Ne_8 helix is 0.0213 ppm. It is comparably small for the Xe@Ne_7 and Xe@Ne_{15} systems discussed in the Appendix.

III. RESULTS AND DISCUSSIONS

A. Xe in Ne_8 helices

In all the tables presented here, the Xe intermolecular shielding tensor is given in terms of the difference between the shielding calculated for the system and that calculated for the Xe atom alone. We have also included both pairs of mirror images. Although this may appear to be redundant, we wished to exhibit the difference in sign of certain off-diagonal elements within enantiomeric pairs.

The Xe shielding tensor components calculated for Xe at the center of a Ne_8 helix where the nuclear site symmetry is C_2 are given in Table I. The number of nonvanishing components of shielding is as predicted by Buckingham and Malm[17] for this nuclear site symmetry. The Xe shielding tensor components for the *R* and *L* helices are related by a rotation that changes the signs of the off-diagonal elements. Three principal components of the tensor and the directions of the principal axes system relative to the laboratory axes are a maximum of six quantities that can be determined from a single crystal NMR experiment. At most three principal components can be obtained from a powder NMR spectrum. Only the isotropic shielding can be obtained from a solution NMR spectrum. We can see from the shielding tensor in Table I that the *R* and the *L* system produce the same Xe NMR spectrum.

TABLE I. The ^{129}Xe shielding tensor components for Xe at the center of a Ne_8 helix (nuclear site symmetry is C_2).

Xe@Ne_8(*R*)			Xe@Ne_8(*L*)		
Full tensor					
−56.4483	0	0	−56.4483	0	0
0	−59.0913	−12.4742	0	−59.0913	12.4742
0	−12.5330	−91.2904	0	12.5330	−91.2904
Symmetric tensor					
−56.4483	0	0	−56.4483	0	0
0	−59.0913	−12.5036	0	−59.0913	12.5036
0	−12.5036	−91.2904	0	12.5036	−91.2904
Antisymmetric tensor					
0	0	0	0	0	0
0	0	+0.0294	0	0	−0.0294
0	−0.0294	0	0	+0.0294	0

TABLE II. The ^{129}Xe shielding tensor for Xe at the center of a $Ne_8 \cdot q_{15}$ helix where the Ne_8 helix is surrounded by a helix of 15 partial charges $(+0.061\,953e)$. Nuclear site symmetry is C_2.

$Xe@Ne_8 \cdot q_{15}(Rr)$ Full tensor			$Xe@Ne_8 \cdot q_{15}(L\ell)$		
−15.6121	0	0	−15.6121	0	0
0	−17.3762	−4.5346	0	−17.3762	4.5346
0	−3.7095	−29.7162	0	3.7095	−29.7162
Symmetric tensor					
−15.6121	0	0	−15.6121	0	0
0	−17.3762	−4.1221	0	−17.3762	4.1221
0	−4.1221	−29.7162	0	4.1221	−29.7162
Antisymmetric tensor					
0	0	0	0	0	0
0	0	−0.4126	0	0	+0.4126
0	+0.4126	0	0	−0.4126	0
$Xe@Ne_8 \cdot q_{15}(R\ell)$ Full tensor			$Xe@Ne_8 \cdot q_{15}(Lr)$		
−14.5921	0	0	−14.5921	0	0
0	−16.9236	−4.1914	0	−16.9236	4.1914
0	−3.8906	−28.3861	0	3.8906	−28.3861
Symmetric tensor					
−14.5921	0	0	−14.5921	0	0
0	−16.9236	−4.0410	0	−16.9236	4.0410
0	−4.0410	−28.3861	0	4.0410	−28.3861
Antisymmetric tensor					
0	0	0	0	0	0
0	0	−0.1504	0	0	+0.1504
0	+0.1504	0	0	−0.1504	0

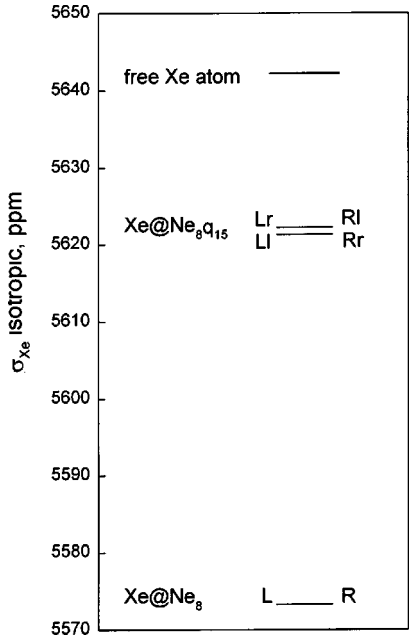

FIG. 1. The isotropic shielding of the Xe atom in a left- or right-handed helix of eight Ne atoms, and in helices of eight Ne atoms and 15 partial positive charges.

B. Xe in diastereomeric helices

It is clear from Eqs. (1)–(6) that one knows that *Ll* and *Rr* are mirror images and *Lr* and *Rl* are mirror images. In the various diastereomers shown in Table II, the ^{129}Xe shielding tensor exhibits the expected sign change for the off-diagonal elements of the full shielding tensor in going from one mirror image to the other. The two diastereomeric pairs are different from each other; all the shielding tensor components are different. For Xe in the $Xe@Ne_8$, the symmetry of the system is such that there is a C_2 axis (chosen as the laboratory X axis) perpendicular to the helical axis, in which case only σ_{YZ} and σ_{ZY} are nonvanishing. Thus one principal axis of the symmetric part of the shielding tensor lies along the X axis of the molecular frame. As expected, the principal components of the symmetric tensor in corresponding systems (R and L, $R\ell$ and Lr, Rr and $L\ell$) are the same. The principal axis system of the tensor does rotate, in going from $Xe@R$ to $Xe@L$, for example. The lower symmetry at the Xe site in $Xe@Ne_7$, $Xe@Ne_7 \cdot q_{13}$ systems, and extension of the helix in the $Xe@Ne_{15}$ system provide some additional information (see the Appendix).

The diastereomers are less deshielded than the L or R systems. The fact that we used positive charges means that the Ne electrons having been drawn toward the positive charges leave the Ne atoms unable to provide as large a shielding response via overlap and exchange with the Xe electrons.

The isotropic chiral shift, the difference between the shieldings in the diastereomeric pairs, is $[\sigma_{iso}(Xe@L\ell) - \sigma_{iso}(Xe@Lr)] = [\sigma_{iso}(Xe@Rr) - \sigma_{iso}(Xe@R\ell)] = 0.9324$ ppm for $Xe@Ne_8 \cdot q_{15}$. The Xe shielding level diagram in Fig. 1 can be viewed as a ^{129}Xe NMR spectrum by viewing the diagram sideways: the enantiomers $Xe@R$ and $Xe@L$ both appearing as one peak, highly deshielded from the gas peak (free Xe atom), and the diastereomers giving rise to the two peaks separated by 0.9342 ppm, each peak comprising of two species, one peak from $Xe@Rr$ and $Xe@L\ell$, the other peak from $Xe@R\ell$ and $Xe@Lr$, still deshielded compared to the Xe gas peak, but not as much.

C. Antisymmetric elements

Although it may come as a surprise to some, the chemical shift tensor is not necessarily a symmetric tensor.[17–19] Experimentally it is difficult to measure the antisymmetric components directly. The symmetric part of the shielding tensor appears in the NMR Hamiltonian as first-order corrections to the Zeeman transition frequency. In the high-field regime where the Zeeman interactions are dominant, these terms remain secular: their typical magnitudes are δ in the order of ppm of the Larmor frequency and are easily measurable by conventional NMR techniques. In contrast, the antisymmetric part of the shielding tensor appears only in the nonsecular spin terms, so their Hamiltonian appears as a second-order effect of the order δ^2. When quadrupolar nuclei are observed, a tilting of the axis of quantization away from the direction of B_0 is brought about by the quadrupolar interaction, which enables nonsecular terms to show up, in particular, for the antisymmetric part of the shielding to manifest itself as a frequency shift in the order of $\delta\omega_Q$, that is of the order of magnitude of ppm of the quadrupole coupling constant, in a single-crystal experiment. The first attempt of a direct measurement that takes advantage of this

is described by Wi and Frydman.[20] ^{131}Xe would be a good candidate. Previous attempts at obtaining the antisymmetric part of the shielding have been through relaxation experiments.[21–23]

Theoretically, the condition for the existence of the antisymmetric component of σ has been studied. In particular, Buckingham carried out an analysis of which nuclear site point-group symmetries support antisymmetry and how many distinct nonvanishing elements are possible.[17] Hansen and Bouman have performed extensive calculations and provided pictorial representations of the antisymmetric part.[19] More recent discussions on the antisymmetric part of the shielding tensor can be found elsewhere.[20,24] The magnitude of the antisymmetry has been linked to strained small rings.[19,25,26] In this paper we discuss antisymmetry in connection with chirality.

There are two theoretical aspects to the existence of antisymmetric components which are of interest. First of all, since the diamagnetic part is symmetric when the gauge origin is taken to be at the nucleus of interest, only the paramagnetic portion of the shielding contributes. Hence the existence of the antisymmetric tensor may be considered a (gauge-dependent) measure of the paramagnetic component. Second, the current induced by the static field must have a component parallel to the magnetic field.[27] Some theories of nuclear magnetic shielding assume the magnetic field and induced current are perpendicular to each other.

All of the above has nothing to do with chirality. Clearly, with the exception of the chiral point groups, D_n, T, and O, which forbid the existence of antisymmetric shielding,[17] chirality is a sufficient condition for the existence of antisymmetry in the shielding but not a necessary condition. It is interesting to note that the creation of diastereomers by the addition of further chiral elements will split the scalar shielding at the center even if the added elements preserve the symmetries listed above. The antisymmetric shielding tensors will still be zero. On the other hand, if the added elements create a lower symmetry than D_n, T, or O, the antisymmetric elements will be created at the center, and of course, be different for the different diastereomers. The splittings that will appear in these cases are the antisymmetric elements of the diastereomers. As discussed earlier, all elements of the shielding tensors are either identical for L and R helices, or differ by a rotation-dependent sign. Isolated atomic Xe is totally diamagnetic; with the origin at the nucleus, there is no paramagnetic shielding. The field-induced current is perpendicular to the external B_0 field. Hence the existence of antisymmetric terms of the shielding tensors for Xe in L or R Ne helices are a measure of a lower symmetry induced paramagnetic shielding and current parallel to the external magnetic field. Since the helical axis is chosen along the Z direction in the molecular frame, the signs of the antisymmetric tensor elements are reversed for the components involving Z, when the handedness of the Ne helix is changed from L to R. Because the C_2 symmetry axis is along the molecular frame x axis for the Xe@Ne_8 system, the only antisymmetric component is $\frac{1}{2}[\sigma_{YZ}-\sigma_{ZY}]$.

We see in Tables I and II that the equivalent antisymmetric terms of $(L\ell)$ and (Lr) are not only shifted from L, but differ from one another. That is,

$$\tfrac{1}{2}[\sigma_{YZ}-\sigma_{ZY}]_L = 0.0294 \text{ ppm},$$

$$\tfrac{1}{2}[\sigma_{YZ}-\sigma_{ZY}]_{L_\ell} = 0.4126 \text{ ppm},$$

$$\tfrac{1}{2}[\sigma_{YZ}-\sigma_{ZY}]_{Lr} = 0.1504 \text{ ppm}.$$

This difference is a direct measure that the paramagnetic shielding and current parallel to the field have a chiral induced character.

In the following paper (Paper II) we investigate the nuclear magnetic shielding tensor of a naked spin interacting with Ne_8 helices and partial charges identical with those coupled to Xe in this paper, as well as partial charges which are negative. The antisymmetric terms in the Xe complexes are an order of magnitude larger than those of the naked spin. Clearly the induced chiral paramagnetic currents of the Xe electrons play a dominant role.

D. Comparison with the pairwise additive model for shielding

The *ab initio* shielding tensors that we have calculated for the systems in this work (Xe@Ne_8 and also the Xe in Ne_7 and Ne_{15} helices that are mentioned in the Appendix) can be understood in terms of an additive model. For the calculations of line shapes of Xe in zeolite channels, one of us has created a ''dimer tensor model'' described in a recent paper.[28] The shielding tensor of a single Xe atom located at a specific position (x_J, y_J, z_J), within a channel constituted of Ne atoms is approximated by a sum of Xe–Ne contributions. In the additive dimer tensor model, the intermolecular Xe shielding is considered to arise from contributions from each atom of the channel by considering each Xe-atom contribution at a time. In other words, it is assumed that the Xe shielding of the Jth Xe atom at position (x_J, y_J, z_J), can be calculated by using a summation over the contributions of Xe–Ne dimers, using the *ab initio* XeNe dimer shielding function[29] in each case. For example, the contribution to the Xe shielding due to ith Ne atom located at (x_i, y_i, z_i) is given by the *ab initio* tensor component, the function $(\sigma_\perp, \sigma_\perp, \sigma_\parallel)_{\mathrm{XeNe}}$ (evaluated at r_{XeNe}). The derived expressions turn out to be very simple geometric factors coupled with $\sigma_\perp$ (evaluated at r_{XeNe}) and $\sigma_\parallel$ (evaluated at r_{XeNe}). For example,

$$\sigma_{XX} = [(x_i - x_J)/r_{iJ}]^2 \sigma_\parallel + \{[(y_i - y_J)/r_{iJ}]^2 + [(z_i - z_J)/r_{iJ}]^2\}\sigma_\perp . \quad (7)$$

$$\tfrac{1}{2}(\sigma_{XY} + \sigma_{YX}) = [(x_i - x_J)/r_{iJ}]\cdot[(y_i - y_J)/r_{iJ}](\sigma_\parallel - \sigma_\perp). \quad (8)$$

Terms like these are summed to include all the atoms in the channel. Then the shielding response in an external magnetic field (B_0) along a particular chosen direction (θ, ϕ),[19] can be calculated as follows:

TABLE III. Comparison of the *ab initio* values of the ^{129}Xe shielding tensor components for Xe inside various Ne_n helices with those calculated using the dimer tensor model in which the tensor components of the supermolecule system ($Xe@Ne_n$) are estimated as sums over the *ab initio* ^{129}Xe–Ne dimer tensor components at various distances. "*Ab initio*" are the values for the $Xe@Ne_n$, "Calc" are the values from the additive dimer tensor model.

	Ab initio	Calc	*Ab*-Calc
$Xe@Ne_7(L)$			
σ_{XX}	−55.4526	−55.3409	−0.11
σ_{YY}	−52.2268	−52.1340	−0.09
σ_{ZZ}	−86.6174	−98.1004	11.48
$\frac{1}{2}(\sigma_{XY}+\sigma_{YX})$	−0.0948	0.0000	−0.09
$\frac{1}{2}(\sigma_{XZ}+\sigma_{ZX})$	−2.8110	−3.2641	0.45
$\frac{1}{2}(\sigma_{YZ}+\sigma_{ZY})$	12.7147	15.4706	−2.76
σ_{iso}	−64.7656	−68.5253	3.76
$Xe@Ne_8(L)$			
σ_{XX}	−56.4270	−56.5864	0.16
σ_{YY}	−59.0700	−59.4600	0.39
σ_{ZZ}	−91.2691	−103.6742	12.41
$\frac{1}{2}(\sigma_{XY}+\sigma_{YX})$	0.0000	0.0000	0.00
$\frac{1}{2}(\sigma_{XZ}+\sigma_{ZX})$	0.0000	0.0000	0.00
$\frac{1}{2}(\sigma_{YZ}+\sigma_{ZY})$	12.5036	15.4706	−2.97
σ_{iso}	−68.9221	−73.2404	4.32
$Xe@Ne_{15}(L)$			
σ_{XX}	−64.8244	−66.4863	1.66
σ_{YY}	−65.1560	−66.6497	1.49
σ_{ZZ}	−97.4705	−111.0832	13.61
$\frac{1}{2}(\sigma_{XY}+\sigma_{YX})$	−0.1955	−0.1000	−0.10
$\frac{1}{2}(\sigma_{XZ}+\sigma_{ZX})$	3.3079	4.2987	−0.99
$\frac{1}{2}(\sigma_{YZ}+\sigma_{ZY})$	6.7964	8.9260	−2.13
σ_{iso}	−75.8170	−81.4067	5.59

$$\sigma_{B0}(\theta,\phi)=\sigma_{XX}\sin^2\theta\cos^2\phi+\sigma_{YY}\sin^2\theta\sin^2\phi+\sigma_{ZZ}\cos^2\theta+\tfrac{1}{2}(\sigma_{XY}+\sigma_{YX})\sin^2\theta\sin 2\phi+\tfrac{1}{2}(\sigma_{XZ}+\sigma_{ZX})\sin 2\theta\cos\phi+\tfrac{1}{2}(\sigma_{YZ}+\sigma_{ZY})\sin 2\theta\sin\phi. \quad (9)$$

Since we have calculated the $Xe@Ne_7$ and $XeNe_8$ and $Xe@Ne_{15}$ using the same basis functions and the same method (DFT-B3LYP) for Xe and Ne as what we had used for $(\sigma_\perp$ and $\sigma_\parallel)_{XeNe}$ (evaluated at r_{XeNe}) in the isolated XeNe dimer, it would be a good test of the dimer tensor model to compare the symmetric part of the tensor predicted using the additive dimer tensors against the *ab initio* shielding tensor for Xe in the helix of Ne atoms. Results are shown in Table III, where the *ab initio* values calculated for the $Xe@Ne_n$ are compared with the values calculated from the additive dimer tensor model.

The additive model works best at longer distances, of course, but it seems to work reasonably well even at Xe–Ne distances well inside the r_{min} (3.8661 Å) of the XeNe potential well. In Table III we see that the dimer tensor model gives a good accounting of the signs and magnitudes of the tensor components: the symmetry of the system is preserved, the signs of the off-diagonal elements are preserved, the nonvanishing off-diagonal symmetric components are nonvanishing, and the magnitudes of the individual components of the symmetric part of the shielding tensor are relatively well reproduced. The differences between *ab initio* and additive model values are found to be reasonably small. The largest error occurs where the deshielding is the greatest; since the axis of the Ne helix is along the *z* axis, this is the *zz* component. Nevertheless, even for this worst case, the relative error is no more than 15%. We also calculated the right-handed ones (not shown), and the sign changes occur just as in the *ab initio* values. The additive tensor model provides the reasoning for the relative magnitudes of the tensor elements. With the helix axis along the *Z*, the largest deshielding component is found to be σ_{zz}, as seen in Tables I–V. Such trends are easily predicted for nanochannels.[28,29]

TABLE IV. The ^{129}Xe shielding tensor components for Xe in a Ne_7 helix. Nuclear site symmetry is C_1.

$Xe@Ne_7(R)$ Full tensor			$Xe@Ne_7(L)$		
−55.4526	−0.1086	2.8242	−55.4526	−0.1086	−2.8242
−0.0810	−52.2268	−12.6953	−0.0810	−52.2268	12.6953
2.7978	−12.7341	−86.6174	−2.7978	12.7341	−86.6174
Symmetric tensor					
−55.4526	−0.0948	2.8110	−55.4526	−0.0948	−2.8110
−0.0948	−52.2268	−12.7147	−0.0948	−52.2268	12.7147
2.8110	−12.7147	−86.6174	−2.8110	12.7147	−86.6174
Antisymmetric tensor					
0	−0.0138	0.0132	0	−0.0138	−0.0132
0.0138	0	0.0194	0.0138	0	−0.0194
−0.0132	−0.0194	0	0.0132	0.0194	0

TABLE V. The ^{129}Xe shielding tensor components for Xe at the center of $Ne_7 \cdot q_{13}$ helices. Nuclear site symmetry is C_1.

$Xe@Ne_7 \cdot q_{13}(Rr)$ Full tensor			$Xe@Ne_7 \cdot q_{13}(L\ell)$		
−21.4184	−0.2301	0.6066	−21.4184	−0.2301	−0.6066
−0.3583	−20.6056	−5.7792	−0.3583	−20.6056	5.7792
−0.1738	−5.0188	−37.3808	0.1738	5.0188	−37.3808
Symmetric tensor					
−21.4184	−0.2942	0.2164	−21.4184	−0.2942	−0.2164
−0.2942	−20.6056	−5.3990	−0.2942	−20.6056	5.3990
0.2164	−5.3990	−37.3808	−0.2164	5.3990	−37.3808
Antisymmetric tensor					
0	0.0641	0.3902	0	0.0641	−0.3902
−0.0641	0	−0.3802	−0.0641	0	0.3802
−0.3902	0.3802	0	0.3902	−0.3802	0
$Xe@Ne_7 \cdot q_{13}(R\ell)$ Full tensor			$Xe@Ne_7 \cdot q_{13}(Lr)$		
−20.5602	−0.0417	0.5125	−20.5602	−0.0417	−0.5125
−0.1546	−19.9772	−5.4787	−0.1546	−19.9772	5.4787
−0.0912	−5.1458	−35.9708	0.0912	5.1458	−35.9708
Symmetric tensor					
−20.5602	−0.0981	0.2107	−20.5602	−0.0981	−0.2107
−0.0981	−19.9772	−5.3123	−0.0981	−19.9772	5.3123
0.2107	−5.3123	−35.9708	−0.2107	5.3123	−35.9708
Antisymmetric tensor					
0	0.0564	+0.3019	0	0.0564	−0.3019
−0.0564	0	−0.1664	−0.0564	0	0.1664
−0.3019	0.1664	0	0.3019	−0.1664	0

IV. CONCLUSIONS

The antisymmetric tensor element, only one for the site symmetry of Xe in the Ne_8 helix, is one measure of the induced chirality. The lowering of symmetry in the Ne_7 helix demonstrates the general three-element antisymmetric part. Incidentally, the calculated *ab initio* Xe shieldings in the Ne_7, Ne_8, and Ne_{15} helices provide a good test of the dimer tensor model. This model provides good estimates for all six elements of the symmetric shielding tensor.

The chiral potential provided by the point charge helix is sufficient to provide a chiral shift for Xe atom that is of the right order of magnitude to be observable in the ^{129}Xe NMR spectrum. Using point charges each about one-tenth of a typical partial charge used for a carbonyl atom in protein dynamics simulations was sufficient to see a chiral shift of the order of 1 ppm. This gives us some hope that we can calculate the Xe shielding at the center of the chiral cryptophane cage attached to chiral tethers by using a chiral potential, point charges to represent the atoms of the tether, (i.e., no additional electrons, no additional basis functions!) so that we might be able to assign the fine structure observed by E. J. Ruiz *et al.* in functionalized Xe.[5]

ACKNOWLEDGMENTS

This work has been supported by The National Science Foundation (Grant No. CHE99-79259). The ideas that led to this work came about in discussions between R.A.H. and C.J.J. while C.J.J. was a Visiting Miller Professor at the University of California, Berkeley. She is grateful for the support of the Miller Research Institute and for the hospitality of Professor Alex Pines. R.A.H. and C.J.J. are grateful to E. Janette Ruiz, Megan M. Spence, and other members of the Pines group for the discussions of their experimental observations which inspired this work. We thank Aage E. Hansen for a careful reading of earlier versions of the manuscripts and his insightful comments and corrections.

APPENDIX: Xe IN Ne_7 AND Ne_{15} HELICES

Since the helix is made up of a small integral number of Ne atoms we use either a full helical turn plus one extra Ne or else not quite a full turn. A full helical turn would have had a half Ne atom at each end! We use seven Ne atoms for not quite a full turn, and eight Ne atoms for a helix with one turn plus one Ne atom. The point-charge helix is chosen in the same way as the Ne_n helix, that is, not quite one full turn, or else one turn plus one extra charge. With seven Ne atoms, we choose 13 positive charges, with eight Ne atoms, 15 positive charges.

Since the helical axis is the *Z* axis, off-diagonal elements involving *Z* reverse sign in going from *R* to *L*. This can be seen in Table IV. This is true also for the $Xe@Ne_8$ and $Xe@Ne_{15}$ systems, except that the *XY* and *YX* elements are zero by symmetry in $Xe@Ne_8$. The lower symmetry at the nuclear site in the $Xe@Ne_7$ system illustrates the most general case. There are six distinct nonvanishing components in the symmetric part and three nonvanishing antisymmetric elements. The lower symmetry also leads to larger antisymmetric terms (see Table V) and the diastereomers of the lower symmetry $Ne_7 \cdot q_{13}$ system leads to a larger shielding difference (chiral shift) than the more symmetrical $Ne_8 \cdot q_{15}$ system.

TABLE VI. Isotropic Xe shielding in various helices.

Model	$Xe@Ne_7 \cdot q_{13}$	$Xe@Ne_8 \cdot q_{15}$	$Xe@Ne_{15}$
L, R	−64.7656	−68.9434	−75.817
Rr, Ll	−26.4683	−20.9015	
Lr, Rl	−25.5027	−19.9673	
(*Ll-Lr*), (*Rr-Rl*)	−0.9656	−0.9342	

The two-turn Ne_{15} helix permits us to explore the effects on the Xe response of extending the helix. The deshielding is greater for the larger number of Ne atoms, in comparing Ne_7, Ne_8, and Ne_{15} (in Table VI). Extending the helix to two turns adds Ne atoms at longer distances from Xe. Since the Xe–Ne deshielding becomes monotonically less pronounced as the r_{XeNe} increases, the dimer tensor model explains why adding more turns to the helix does not produce a deshielding proportional to the incremental number of neon atoms.

[1] E. L. Eliel and S. H. Wilen, *Stereochemistry of Organic Compounds* (Wiley, New York, 1994).
[2] W. Moffitt and A. Moscowitz, J. Chem. Phys. **30**, 648 (1959).
[3] K. Bartik, M. El-Haouaj, M. Luhmer, A. Collet, and J. Reisse, ChemPhysChem **1**, 221 (2000).
[4] K. Bartik, M. Luhmer, A. Collet, and J. Reisse, Chirality **13**, 2 (2001).
[5] E. J. Ruiz, M. M. Spence, S. M. Rubin, D. E. Wemmer, A. Pines, N. Winssinger, F. Tian, S. Q. Yao, and P. G. Schultz, *43rd Experimental NMR Conference*, April 14–19, 2002, Asilomar, CA.
[6] M. M. Spence, S. M. Rubin, I. E. Dimitrov, E. J. Ruiz, D. E. Wemmer, A. Pines, S. Q. Yao, F. Tian, and P. G. Schultz, Proc. Natl. Acad. Sci. U.S.A. **98**, 10654 (2001).
[7] W. D. Cornell, P. Cieplak, C. I. Bayly *et al.*, J. Am. Chem. Soc. **117**, 5179 (1995).
[8] W. N. Lipscomb, Adv. Magn. Reson. **2**, 137 (1966).
[9] T. Helgaker, M. Jaszunski, and K. Ruud, Chem. Rev. **99**, 293 (1999).
[10] F. A. Hamprecht, A. J. Cohen, D. J. Tozer, and N. C. Handy, J. Chem. Phys. **109**, 6264 (1998).
[11] A. C. de Dios and C. J. Jameson, J. Chem. Phys. **107**, 4253 (1997).
[12] C. J. Jameson, D. N. Sears, and A. C. de Dios, J. Chem. Phys. **118**, 2575 (2003).
[13] H. Partridge and K. Faegri, Jr., NASA Tech. Memo. 103918 (1992).
[14] D. M. Bishop and S. M. Cybulski, Chem. Phys. Lett. **211**, 255 (1993).
[15] M. J. Frisch, G. W. Trucks, H. B. Schlegel *et al.*, GAUSSIAN 98, Revision A.9, Gaussian, Inc., Pittsburgh, PA, 1998.
[16] S. F. Boys and F. Bernardi, Mol. Phys. **19**, 538 (1970).
[17] A. D. Buckingham and S. Malm, Mol. Phys. **22**, 1127 (1971).
[18] R. F. Schneider, J. Chem. Phys. **48**, 4905 (1968).
[19] A. E. Hansen and T. D. Bouman, J. Chem. Phys. **91**, 3552 (1989).
[20] S. Wi and L. Frydman, J. Chem. Phys. **116**, 1551 (2002).
[21] R. M. Lynden-Bell, Mol. Phys. **29**, 301 (1975).
[22] F. A. L. Anet, D. J. O'Leary, C. G. Wade, and R. D. Johnson, Chem. Phys. Lett. **171**, 401 (1990).
[23] J. Kowalewski and L. Werbelow, J. Magn. Reson. **128**, 144 (1997).
[24] F. A. L. Anet, Concepts Magn. Reson. **3**, 193 (1991).
[25] A. L. Barra and J. B. Robert, Chem. Phys. Lett. **136**, 224 (1987).
[26] C. M. Smith, R. D. Amos, N. C. Handy, Mol. Phys. **77**, 381 (1992).
[27] J. Herzfeld, D. J. Olbris, E. Furman, and V. Benderskiy, J. Chem. Phys. **113**, 5162 (2000).
[28] C. J. Jameson, J. Chem. Phys. **116**, 8912 (2002).
[29] C. J. Jameson, J. Chem. Phys. **116**, 3805 (2002).